



## THE TOUGHENING EFFECT OF MICROSCOPIC FILAMENT MISALIGNMENT ON MACROSCOPIC BALLISTIC FABRIC RESPONSE

T. I. Zohdi and D. J. Steigmann

*Department of Mechanical Engineering*

*6195 Etcheverry Hall*

*University of California, Berkeley, CA, 94720-1740, USA*

*email: zohdi or steigman@newton.berkeley.edu, fax. 510-642-5539*

**Abstract.** Typically the observed rupture of a woven fabric is not abrupt, but has a period of decay or “softening”. One source of this interval is the misalignment of the filaments in the fabric, which leads to locally inhomogeneous rupture that manifests itself as gradual macroscopic failure. In this communication, we investigate the effect of microstructural misalignment on the failure of filament bundles used in lightweight ballistic shielding, and its consequent toughening effect.

**1. Introduction.** During the past three decades, lightweight ballistic fabric has owed its success largely to the incorporation of high strength fibers. Applications range from body armor to the protection of mission-critical military and commercial structural components. For overviews, recent applications, models, and case studies see Roylance and Wang [3], Taylor and Vinson [8], Shim et al. [4], Shockey et al. [5], Johnson et al. [1], Tabiei and Jiang [7] Kollegal and Sridharan [2], Simons et al. [6] and Walker [10]. In this communication we develop a simple model to extract the aggregate macroscopic behavior of a bundle of microfilaments, which make up a single yarn or fiber in the fabric. As indicated in the abstract, filament misalignment is largely responsible for controlling the gradual decay, as opposed to abrupt rupture, in the macroscopic response (Figure 1). This is due to inhomogeneous individual filament rupture. Here we study the effect of misalignment of microscopic filaments on the aggregate macroscopic energy absorbing capabilities of ballistic fabric.

**2. Microfilament responses.** Since the axial strains are expected to be in the range of 2 %-10 % before rupturing, we consider a Kirchhoff-St. Venant material. The stored energy function for such a material is  $W(\mathbf{E}) = \frac{1}{2} \mathbf{E} : \mathbf{I}\mathbf{E}^Y : \mathbf{E}$ , where  $\mathbf{I}\mathbf{E}^Y$  is the elasticity tensor,  $\mathbf{E} \stackrel{\text{def}}{=} \frac{1}{2}(\mathbf{C} - \mathbf{1})$  is the Green-Lagrange strain,  $\mathbf{C} \stackrel{\text{def}}{=} \mathbf{F}^T \cdot \mathbf{F}$  is the right Cauchy-Green strain,  $\mathbf{F} = \nabla_{\mathbf{X}} \mathbf{x}$  is the deformation gradient and where  $\mathbf{X}$  are referential and  $\mathbf{x}$  are current coordinates respectively. Since the second Piola-Kirchhoff stress can be expressed as  $\mathbf{S} = \frac{\partial W}{\partial \mathbf{E}}$ , we may write  $\mathbf{S} = \mathbf{I}\mathbf{E}^Y : \mathbf{E}$ . After  $\mathbf{S}$  has been computed one may write  $\boldsymbol{\sigma} = \frac{1}{J} \mathbf{F} \cdot \mathbf{S} \cdot \mathbf{F}^T$ ,  $\boldsymbol{\sigma}$  being the Cauchy stress, where  $J$  is the Jacobian of  $\mathbf{F}$ ,  $J = \det \mathbf{F}$ . In many applications, ballistic shielding fabrics are employed in high and low temperature environments. For moderate deformations, a relatively simple thermo-elastic decomposition of the deformation into elastic and thermal components is  $\mathbf{E} = \mathbf{E}_e + \mathbf{E}_\theta$ , where  $\mathbf{E}_e$  is the elastic part of the Green-Lagrange strain and  $\mathbf{E}_\theta$  is the thermal part. A standard procedure is to write a (pseudo) stored energy function in terms of the elastic part of the deformation,  $\hat{W}(\mathbf{E}_e(\mathbf{E}))$ , and thereafter to differentiate in order to determine  $\mathbf{S} = \frac{\partial \hat{W}(\mathbf{E}_e(\mathbf{E}))}{\partial \mathbf{E}}$ .

Following this procedure one writes  $\hat{W}(\mathbf{E}_e) = \frac{1}{2}(\mathbf{E} - \mathbf{E}_\theta) : \mathbf{I}\mathbf{E}^Y : (\mathbf{E} - \mathbf{E}_\theta) + \rho_o H \theta$ , where  $\rho_o$  is the density in the referential configuration and  $H$  is the heat capacity. A common choice for the thermal component is  $\mathbf{E}_\theta = \alpha(\theta - \theta_R)\mathbf{1}$ , where  $\theta_R$  is a reference temperature, since this expression reduces to the commonly used  $\epsilon_\theta = \alpha(\theta - \theta_R)\mathbf{1}$  at infinitesimal deformations. Accordingly,  $\mathbf{S} = \mathbf{I}\mathbf{E}^Y : (\mathbf{E} - \alpha(\theta - \theta_R)\mathbf{1})$ . Our model also employs a thermally-dependent Young's modulus,  $E^Y(\theta)$ , and a thermally-dependent critical rupture stress,  $\sigma^{crit}(\theta)$ . For the polymer used in the upcoming simulations, PBO Zylon, which is produced by the Toyobo Corporation (Toyobo [9]) and which has recently been applied by SRI to ballistic shielding of aircraft (Shockey et al. [5], Simons et al. [6]), we have approximately linear thermal dependency relations

$$\begin{aligned} E^Y(\theta) &= \frac{E_f^Y - E_o^Y}{\theta_f - \theta_o}(\theta - \theta_o) + E_o^Y, \\ \sigma^{crit}(\theta) &= \frac{\sigma_f^{crit} - \sigma_o^{crit}}{\theta_f - \theta_o}(\theta - \theta_o) + \sigma_o^{crit}, \end{aligned} \quad (1)$$

where  $E_o^Y \stackrel{\text{def}}{=} E^Y(\theta_o)$ ,  $E_f^Y \stackrel{\text{def}}{=} E^Y(\theta_f)$ ,  $\sigma_o^{crit} \stackrel{\text{def}}{=} \sigma^{crit}(\theta_o)$  and  $\sigma_f^{crit} \stackrel{\text{def}}{=} \sigma^{crit}(\theta_f)$  are measured data at temperatures  $\theta_o$  and  $\theta_f$ .

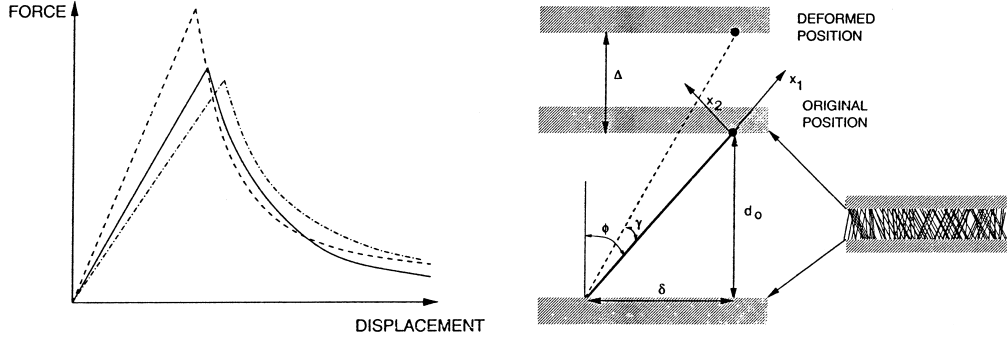


Figure 1: LEFT: A typical macroscopic response for a group of filaments that are not perfectly aligned. RIGHT: A geometrical description of the deformation of an individual filament.

**3. Extraction of axial responses.** Due to the thinness of the filaments, we assume a plane uniaxial-stress type condition. We align the coordinate system with the undeformed axial ( $x_1$ ) state, where  $C_{11}$  is the component of  $\mathbf{C}$  along the length of the filament (Figure 1). Due to the assumption regarding the stress state,  $S_{22} = S_{33} = 0$ . Because the material is assumed to be isotropic, this implies that the Cauchy stress, written in terms of a coordinate system where one axis is aligned with the deformed axial direction of the filament, also has only one nonzero component. By setting  $S_{22} = S_{33} = 0$ , one obtains relations for  $C_{22} = C_{33}$  in terms of  $C_{11}$ . Assuming that the material is isotropic we have

$$\begin{aligned}
E_{11} &= \frac{S_{11}}{E^Y} - \nu \left( \frac{S_{22} + S_{33}}{E^Y} \right) + E_\theta, \\
E_{22} &= \frac{S_{22}}{E^Y} - \nu \left( \frac{S_{11} + S_{33}}{E^Y} \right) + E_\theta, \\
E_{33} &= \frac{S_{33}}{E^Y} - \nu \left( \frac{S_{11} + S_{22}}{E^Y} \right) + E_\theta.
\end{aligned} \tag{2}$$

Enforcing  $S_{22} = S_{33} = 0$ , one obtains

$$\begin{aligned}
S_{11} &= E^Y (E_{11} - \alpha(\theta - \theta_R)), \\
E_{22} &= -\nu (E_{11} - \alpha(\theta - \theta_R)) + \alpha(\theta - \theta_R) = E_{33}.
\end{aligned} \tag{3}$$

Consequently

$$[C] \stackrel{\text{def}}{=} \begin{bmatrix} C_{11} & 0 & 0 \\ 0 & C_{22} & 0 \\ 0 & 0 & C_{33} \end{bmatrix}, \tag{4}$$

where  $C_{22} = -\nu (C_{11} - 1 - 2\alpha(\theta - \theta_R)) + 2\alpha(\theta - \theta_R) + 1 = C_{33}$ , and thus

$$J = \sqrt{C_{11}C_{22}C_{33}} = \sqrt{C_{11}(-\nu(C_{11} - 1 - 2\alpha(\theta - \theta_R)) + 2\alpha(\theta - \theta_R) + 1)^2}. \tag{5}$$

We may decompose the deformation gradient into a rotation and stretch,  $\mathbf{F} = \mathbf{R} \cdot \mathbf{U}$ . Explicitly, for an individual filament we have  $U_{11} = U_i = \frac{L^i}{L_o^i}$ ,  $U_{22} = \sqrt{C_{22}}$ ,  $U_{33} = \sqrt{C_{33}}$ , where  $L^i$  is the deformed length of the filament, and  $L_o^i$  is its original length. Explicitly, the axial stretch is

$$U_i = \frac{L^i}{L_o^i} = \frac{\sqrt{(d_o + \Delta)^2 + \delta_i^2}}{\sqrt{d_o^2 + \delta_i^2}}, \tag{6}$$

where we define the initial nominal gap length by  $d_o$  and the misalignment length by  $\delta_i$  (Figure 1). The misalignment angle  $\phi_i = \cos^{-1} \left( \frac{d_o + \Delta}{L^i} \right)$ , where  $\Delta$  is the applied (vertical) displacement of the gap, will be incremented later in the simulations (Figure 1). Explicitly we may write for the Cauchy stress

$$\begin{aligned}
\begin{bmatrix} \sigma_{11} & \sigma_{12} & \sigma_{13} \\ \sigma_{21} & \sigma_{22} & \sigma_{23} \\ \sigma_{31} & \sigma_{32} & \sigma_{33} \end{bmatrix} &= \frac{1}{J} \begin{bmatrix} \cos(\gamma) & -\sin(\gamma) & 0 \\ \sin(\gamma) & \cos(\gamma) & 0 \\ 0 & 0 & 1 \end{bmatrix} \begin{bmatrix} U_{11} & 0 & 0 \\ 0 & U_{22} & 0 \\ 0 & 0 & U_{33} \end{bmatrix} \begin{bmatrix} S_{11} & 0 & 0 \\ 0 & 0 & 0 \\ 0 & 0 & 0 \end{bmatrix} \times \\
&\quad \begin{bmatrix} U_{11} & 0 & 0 \\ 0 & U_{22} & 0 \\ 0 & 0 & U_{33} \end{bmatrix} \begin{bmatrix} \cos(\gamma) & \sin(\gamma) & 0 \\ -\sin(\gamma) & \cos(\gamma) & 0 \\ 0 & 0 & 1 \end{bmatrix} \tag{7}
\end{aligned}$$

For the axial stress, needed to compute rupture, one can simply re-write the stress tensor with respect to axes that are aligned with the deformed configuration,  $\hat{\sigma} = \mathbf{R}(-\gamma) \cdot \boldsymbol{\sigma} \cdot \mathbf{R}^T(-\gamma)$ . All components of  $\hat{\sigma}$  are zero except the axial component, which is simply  $\sigma^a = \frac{1}{J} U_{11}^2 S_{11}$ .

**4. Aggregate filament bundle responses.** In order to obtain statistically representative results, we consider a large number of filaments (10000) whose misalignment is characterized by a (bounded) distribution  $\phi_o r_i$ ,  $i = 1, 2, \dots, N$ , where the  $r_i$  are random numbers such that  $-1 \leq r_i \leq 1$ , and where  $\phi_o$  is an angular (inclination) control parameter. Algorithmically, for a given filament distribution, the nominal macroscopic vertical displacement is incremented,  $d = d_o + \Delta$ , and the axial Cauchy stress ( $\sigma^a$ ) is checked in each filament. If the axial Cauchy stress exceeds a critical value,  $\sigma^{crit}$ , then the filament is deemed to be ruptured, and it is thrown out of the computation, and all subsequent computations. To illustrate the characteristics of the model, we used material parameters for Zylon, taken from a recent technical report Toyobo [9]:  $E_o^Y = 285$  GPa,  $E_f^Y = 216$  GPa,  $\sigma_o^{crit} = 5.70$  GPa,  $\sigma_f^{crit} = 2.85$  GPa,  $\alpha = -6 \times 10^{-6}$ ,  $\theta_R = 273.13$  °K,  $\theta_o = 303.13$  °K and  $\theta_f = 673.13$  °K. The results for the aggregate absorbed energy, denoted  $\Pi$ , normalized by the total length of the filaments used in the fabric ( $\mathcal{L} \stackrel{\text{def}}{=} \sum_{i=1}^N L_o^i$ ),

$$\Pi = \frac{1}{\mathcal{L}} \sum_{i=1}^N W_i^{MAX} \quad (8)$$

where  $W_i^{MAX} = \frac{EL_o^i}{2}((U_i^{MAX})^2 - 1)^2$  is the maximum stored mechanical energy in the  $i$ th filament attained before rupture, are depicted in Figure 2 for  $N = 10000$  starting filaments. The quantity  $\Pi$  represents the total energy dissipated, up to and including the current state of deformation. Also, in Figure 2, the total (normalized) vertical projection of the axial Cauchy stress,  $\frac{1}{N} \sum_{i=1}^{N_f} \sigma_i^{a,MAX} \cos(\phi_i - \gamma_i)$ , versus the displacement is shown, where  $N_f$  is the number of active (non-ruptured) fibers remaining at the current stage of deformation. The initial length was set to  $d_o = 0.001$  m, with load increments of  $\Delta = 0.000001$  m. The results changed negligibly for finer discretizations. The final nominal length was  $d_f = 0.00105$  leading to nominal stretches of 1.05. The individual filaments rupture when their axial strains attain approximately 2%. During the course of the loading, the upper limit on the individual axial stresses dictates the number of active remaining filaments, and thus the individual filament stored energy maxima ( $W_i^{MAX}$ ). For comparison purposes, filaments with a uniform alignment, i.e. not a distribution, but with all filaments inclined at  $\phi_o$ , were also tested. Referring to Figure 2, when no upper limit is placed on the axial stress, one observes that nonuniform misalignment produces a tougher material, relative to the perfectly aligned filament case, at every angle of inclination. When an upper stress limit is in place, for inclination angles below approximately  $45^\circ$ , the energy absorption is more or less the same for aligned and misaligned configurations, although, for the uniformly aligned case, the behavior is a nonmonotonic function of  $\phi_o$ . This rather small nonmonotonicity, which has been observed by Toyobo [9], is partly due to the fact that the axial Cauchy stress ( $\sigma^a$ ) is a nonmonotone function of  $\phi_o$ , primarily due to the  $\frac{1}{f}$  dependency ( $\sigma^a = \frac{1}{f} U_{11}^2 S_{11}$ ). For inclination angles above approximately  $45^\circ$ , the energy absorption capabilities

of the misaligned configuration are much greater than the aligned configurations. Furthermore, it is stiffer in an overall sense (Figure 2). In the case where upper stress limits are in place, one can interpret the individual ruptures as occurring inhomogeneously, thus making the macroscopic energy absorption of the material greater. *Introducing misalignment is desirable, since it will macroscopically toughen a fabric.* The authors are currently investigating whether such induced misalignment is feasible during the manufacturing of such materials.

**Acknowledgment:** The first author expresses gratitude for support from FAA grant number 01-C-AW-WISU. The second author is grateful for support from the Powelly fund for ballistics research.

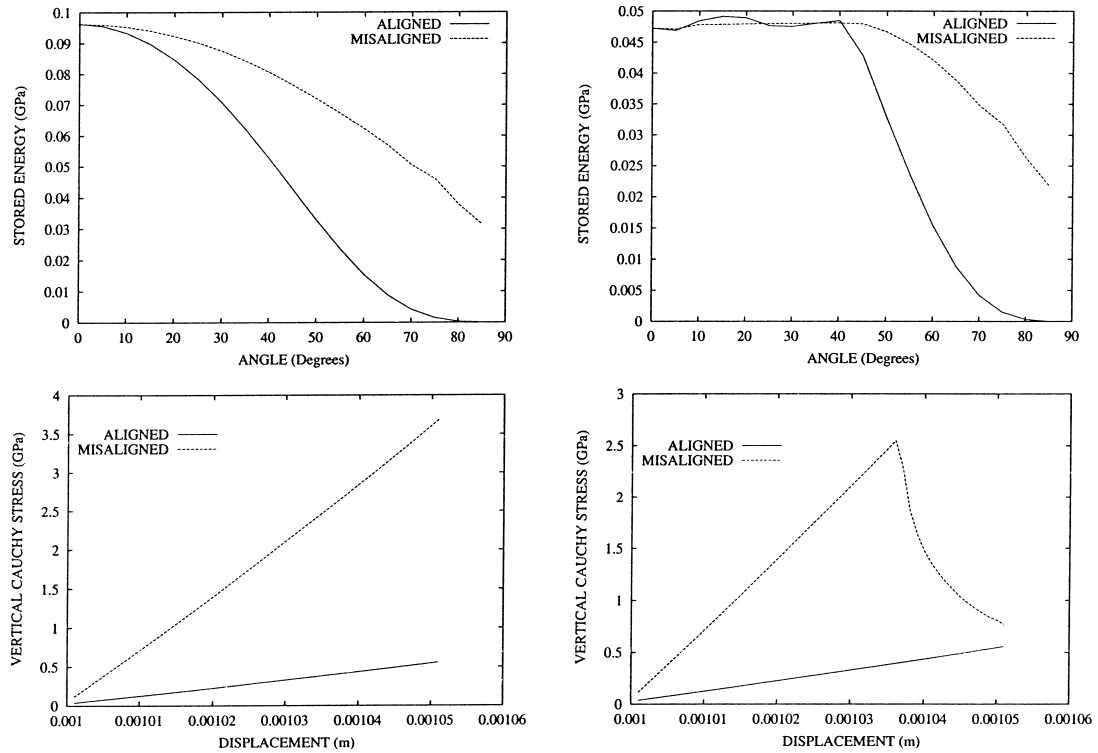


Figure 2: The aggregate absorbed (dissipated) elastic energy of 10000 fibers at 323 °K versus inclination angle for  $\frac{d_f}{d_o} = 1.05$ , without (TOP LEFT) and with upper stress limits (TOP RIGHT). The aggregate vertical projection of the axial Cauchy stress versus displacement  $d$  for an angle of  $\phi_o = 70^\circ$ , without (BOTTOM LEFT) and with upper stress limits (BOTTOM RIGHT).

## REFERENCES

1. Johnson, G. R., Beissel, S. R., and Cunniff, P. M., (1999) A computational model for fabrics subjected to ballistic impact. In *Proceedings of the 18th international symposium on ballistics*, San Antonio, TX, 962-969.
2. Kollegal, M. G. and Sridharan (2000). Strength prediction of plain woven fabrics. *Journal of Composite Materials*. **34**, 240-257.
3. Roylance, D. and Wang, S. S. (1980). *Penetration mechanics of textile structures, ballistic materials and penetration mechanics*. 273-293, Elsevier.
4. Shim, V. P., Tan, V. B. C. and Tay, T. E. (1995). Modelling deformation and damage characteristics of woven fabric under small projectile impact. *Int. J. Impact Engng.* **16**, 585-605.
5. Shockey, D. A., Erlich, D. C. and Simons, J. W. (1999) Lightweight fragment barriers for commercial aircraft. In *Proceedings of the 18th international symposium on ballistics*, San Antonio, TX., 1192-1199.
6. Simons, J. W., Erlich, D. C. and Shockey, D. A. (2001) Finite element design model for ballistic response of woven fabrics. In *Proceedings of the 19th international symposium on ballistics*, Interlaken, Switzerland, 1415-1422.
7. Tabiei, A. and Jiang, Y. (1999). Woven fabric composite material model with material nonlinearity for finite element simulation. *Int. J. of Solids and Structures*. **36**, 2757-2771.
8. Taylor, W. J. and Vinson J. R. (1990). Modelling ballistic impact into flexible materials. *AIAA Journal*, **28**, 2098-2103.
9. Toyobo (2001). PBO fiber ZYLON. Technical Report of the Toyobo Corporation, LTD, <http://www.toyobo.co.jp>.
10. Walker, J. D. (1999). Constitutive model for fabrics with explicit static solution and ballistic limit. In *Proceedings of the 18th international symposium on ballistics*, San Antonio, TX, 1231-1238.